Development of a Stirling Cryocooler Model that Includes a Full Simulation of the Appendix Gap

T. Rawlings, M. Crook, M. Hills

STFC Rutherford Appleton Laboratory
Harwell, Oxford, UK

ABSTRACT

A new Stirling cryocooler model has been developed at the Rutherford Appleton Laboratory. This one-dimensional, finite difference model is able to simulate single and two-stage cryocoolers. The model uses the latest friction factor and heat transfer correlations from the literature and simulates turbulence generation and thermal penetration depths. It runs fast enough to be useful for optimisation, thanks to a robust artificial convergence technique. The model includes a full representation of the cold head, including the displacer motion and the flow past the displacer; this enables the optimisation of certain parameters that could not be assessed previously. The model has been validated against single and two-stage coolers and has been used to investigate changing the cold finger geometry of a single-stage cooler.

INTRODUCTION

A new Stirling cryocooler model has been developed that will be used to optimise the design of the single and two-stage coolers that are produced at the Rutherford Appleton Laboratory (RAL). These coolers are typically designed for use in spacecraft and use flexure bearings and non-contact clearance seals in order to achieve a long lifetime.

Stirling cryocoolers are difficult to model using commercially available 2D or 3D computational fluid dynamics software. The compressible gas, moving mesh and the variable regenerator temperatures make a 2D or 3D model computationally expensive.[1] The approach commonly used by other researchers is to simulate the machine as a network of one dimensional flow paths.[2, 3, 4] Empirical relationships are used to calculate the heat transfer rates and friction factors at different points in the cooler. These models are categorised as third-order[5] and this is the approach used by the new RAL model. The new model is able to run fast enough to be able to optimise over a wide parameter range while still being accurate enough to give useful results.

Most of the third-order models in the literature do not simulate the motion of the displacer; instead, they change the volume of the cells at either end. The RAL third-order model is able to account for the relative motion between the displacer and the cold finger tube and this allows it to simulate effects such as shuttle losses as part of the thermodynamic cycle.

MODEL OUTLINE

The model has been developed using MATLAB. The different regions of the cooler are split up into cells and the finite difference method is used to create a system of ordinary differential

Cryocoolers 21, edited by R.G. Ross, Jr., J.R. Raab and S.D. Miller

equations. For the gas cells, the mass, energy, momentum and turbulence state are tracked over time and, for solid cells, the temperature is tracked. The model solves the differential equations by using a backwards differentiation formula. It runs until the relative changes in the solid cell temperatures over a cycle are below a threshold. The rate of convergence is accelerated by using a method that artificially adjusts the temperatures.

Discretisation

The model splits the cooler into cells, as shown in Figure 1. The Eulerian approach is used, where the cells are fixed relative to the cooler geometry, because different regions can have very different friction factor and heat transfer correlations. The mass and energy equations are evaluated for each gas cell and the momentum equations are evaluated at the nodes between the cells. This is known as the staggered grid technique and helps to keep the simulation stable.[6]

The model uses branching flow paths to simulate appendix gaps, compressor and displacer backshells and the first stage outlet of two-stage coolers. Mass and energy can be transferred between flow paths but momentum is not transferred.

The model simulates the entire cold finger as one system so it is not modular. However, it can be configured to simulate one or two stages of cooling; it allows for optional heat exchanger regions and provides the option to split the regenerator into sections with different properties.

Model Equations

Gas Cells. The rate of change of the mass and energy of each gas cell (i) is given by the following differential equations, derived from the laws of conservation of mass and energy. The rate of change in mass is simply the difference between the mass flow rates at the nodes (j).

$$\frac{dm_i}{dt} = \dot{m}_{j-1} - \dot{m}_j \tag{1}$$

The energy of the gas is the sum of its internal and kinetic energy. The equation for the

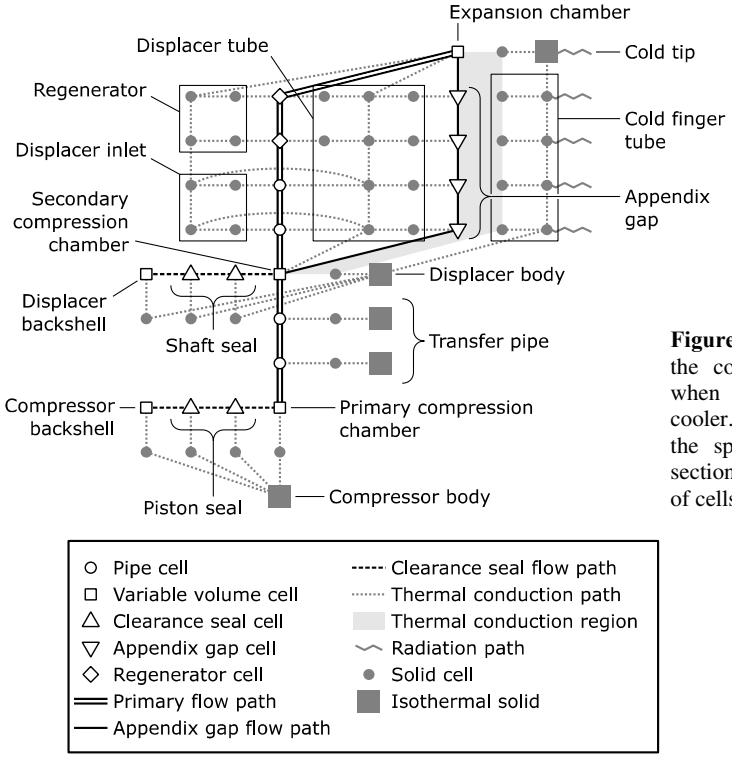

Figure 1. A schematic showing the connections between cells when simulating a single-stage cooler. It is possible to adjust the spatial resolution of each section by adjusting the number of cells.

rate of change of energy accounts for the energy carried by the gas, the flow work, the mechanical work done on the gas, the thermal conduction within the gas and the rate of heat transfer between the gas and its surroundings.

$$\frac{dE_i}{dt} = \dot{E}_{advection_i} + \dot{W}_{flow_i} + \dot{W}_{mechanical_i} + \dot{Q}_{conduction_i} + \dot{Q}_{transfer_i} \tag{2}$$

To convert from masses and energies to temperatures and pressures, the model can either use the ideal gas equation of state or can simulate real gas effects by using a 2D look-up table generated using REFPROP.[7]

The differential equation for the rate of change of momentum at each node is derived from the law of momentum conservation. It accounts for the momentum carried by the gas, the pressure forces, minor losses due to changes in flow area and any frictional forces.

$$\frac{dp_j}{dt} = \dot{p}_{flow_j} + F_{pressure_j} + F_{minor_j} + F_{friction_j} \tag{3}$$

In addition to mass, energy and momentum, the model keeps track of the level of turbulence for some of the cells. For the transfer pipe and other ducts, the mass of gas that is turbulent is tracked.

$$\frac{dm_{\mathcal{T}_i}}{dt} = \dot{m}_{\mathcal{T}_{advection_i}} + \dot{m}_{\mathcal{T}_{generation_i}} + \dot{m}_{\mathcal{T}_{decay_i}} \tag{4}$$

For variable volume cells such as the compression and expansion chambers, the turbulence kinetic energy is tracked.

$$\frac{dK_i}{dt} = \dot{K}_{advection_i} + \dot{K}_{decay_i} \tag{5}$$

Solid Cells. The equation for the rate of change of the thermal energy of the solid cells accounts for conduction between neighboring cells, heat transfer with the gas and thermal radiation. The temperature of each cell can then be calculated from the cell energy.

$$\frac{dE_{s_i}}{dt} = \dot{Q}_{s_{axial_i}} + \dot{Q}_{s_{radial_i}} + \dot{Q}_{s_{transfer_i}} + \dot{Q}_{s_{radiation_i}} \tag{6}$$

Interpolation

To calculate the energy of the gas that is flowing in and out of each gas cell, it is necessary to know the pressures and temperatures of the gas at the boundaries of the cell. Calculating the boundary temperature by simply averaging the temperatures of the neighbouring cells can result in the model producing unphysical temperature oscillations. This is because averaging causes the temperature of the downwind cell to affect the temperature of the gas flowing into it.

A number of different interpolation methods were tested to determine which was able to remove the unphysical oscillations and produce an accurate result with the fewest cells. The QUICK scheme was selected.[8] This is a blend of the average of the neighbouring cell temperatures and an extrapolated temperature from the upwind cells. Simple averages were used for the pressures at the nodes and the velocities at the cell centres as these did not cause oscillations.

Numerical Method

Explicit and implicit solvers were investigated to determine which type was fastest at solving the model's system of differential equations. Explicit solvers must take time steps that are shorter than the time taken for a pressure wave to cross each model cell. This is known as the Courant-Friedrichs-Lewy condition.[9] Implicit solvers are more computationally expensive per step but are not affected by this condition and so are able to take much longer time steps. The overall simulation time was significantly reduced by using an implicit solver. MATLAB's ode15s solver was selected.[10] The backward differentiation formula option was used and the order was set to two to improve its stability.

Convergence Acceleration

The model will naturally approach a periodic steady state where the temperatures at the end of each cycle are the same as the temperatures at the start of the cycle. The model is deemed to have converged when the following condition is met for every solid cell:

$$\frac{|T_{end} - T_{start}|}{T_{end}} < 10^{-6} \tag{7}$$

It can take thousands of cycles for the model to converge naturally. This is because the regenerator mesh cells typically have a much higher heat capacity than the gas passing through them, so it takes many cycles to change the mesh cell temperature. To speed up convergence, Stirling cycle models typically use convergence acceleration methods.

The RAL third-order model combines two techniques: energy flow equalisation and cell temperature adjustment. Using both of these techniques produces a convergence acceleration method that is fast and robust.

Energy flow equalisation. This method has been previously used in the Stirling cycle models of Kühl[11] and Harvey.[12] For a single-stage cooler, it can be assumed that energy only enters or leaves the cold finger at either end. This means that the energy flowing along the cold finger over a cycle must be the same along its length when the model is converged. If this is not the case, the model calculates and applies adjustments to the cell temperatures in order to make the energy flow uniform. The required adjustments vary along the length of the cold finger but the same adjustment is applied to all the cells that are at the same axial position (each row of cells in Figure 1).

Cell temperature adjustment. This method has been used in the Stirling engine model of Urieli.[2] It accelerates the rate of convergence by multiplying the natural temperature change of each cell over the previous cycle by a factor (a) and adding this to the current cell temperature.

$$T_{new} = T_{end} + a(T_{end} - T_{start}) \tag{8}$$

These two methods are effective in different situations. If the cells are well connected thermally, the energy flow equalisation technique can be used because a temperature change of one cell will strongly affect the energy flow to neighbouring cells. This occurs if the regenerator is effective because the temperature of a regenerator cell strongly affects the temperature of the gas flowing through it. If the regenerator is ineffective, temperature changes of cells have little impact on their neighbours and the cell temperature adjustment technique works better.

The model combines the temperature perturbations predicted by these two convergence methods. The cell temperature adjustment perturbations are scaled so that the largest of these perturbations is half the magnitude of the largest energy flow equalisation perturbation. The perturbations for each cell are then added together. To keep the convergence stable, the sum of these perturbations is multiplied by a scale factor before being applied. This scale factor is reduced when necessary to ensure that the largest temperature perturbation does not exceed 5 K. The scale factor is also reduced if the model is not converging because the applied temperature changes are oscillating. The convergence acceleration method is applied every two cycles. The model typically converges in less than 300 cycles which takes approximately four hours on a desktop PC. Multiple cases can be run in parallel by using MATLAB's Parallel Computing Toolbox.

MODEL FEATURES

Solid Surface Temperature

The model tracks the surface temperatures of the solid components separately to their interior temperatures. This reduces the rate of heat transfer, particularly if the solid is a good insulator.

In regions such as the compression chamber, the interior of the chamber wall is assumed to be isothermal. If a sinusoidal heat transfer rate ($\dot{Q} = \dot{Q}_A e^{i\omega t}$) is applied, the wall surface temperature variation (T_W) lags the heat transfer rate by 45°,

$$\frac{T_W}{\dot{Q}} = \frac{\delta}{kA_{gs}(1+i)} \tag{9}$$

where A_{gs} is the surface area, $\delta = \sqrt{2k/(\omega\rho c)}$ is the thermal penetration depth, ω is the angular frequency, k is the conductivity, ρ is the density and c is the specific heat capacity.[13, 4] To simulate this, the model uses the method developed by Kühl.[11] An extra solid cell is added to represent the wall surface and the thermal mass of this extra cell and the resistance between it and the isothermal region are chosen so that the temperature of the cell matches T_W. This is known as a lumped-capacitance model. The thermal mass of the cell must be $C_W = \frac{1}{2}\delta A_{gs}\rho c$ and the thermal resistance must be $R = \delta/(k\, A_{gs})$.

This method has been extended so that the model can also simulate solids of a finite thickness (r) where the temperature of the interior can change. This is particularly important when simulating the regenerator mesh. The surface temperature is then given by equation 10.[13, 4]

$$\frac{T_W}{\dot{Q}} = \frac{\delta}{kA_{gs}(1+i)} \; \frac{1}{\tanh\left(\frac{r}{\delta}(1+i)\right)} \tag{10}$$

By using two solid cells, one representing the wall surface and one representing the interior, it is possible to ensure that the surface temperature in the model responds in the same way as the theoretical surface temperature. The thermal masses of the two cells and the resistance between them is selected so that the response matches equation 10.

Appendix Gap Heat Transfer

The appendix gap is the region between the displacer tube and the cold finger tube. The long-life coolers developed at RAL do not use dynamic seals so require a small appendix gap to reduce the flow of gas past the displacer. However, if the gap is too small, the level of shuttle losses is increased. Shuttle losses occur due to the relative motion of the displacer and cold finger tube. As the displacer and cold finger tube move past each other, their thermal gradients become offset. Thermal energy conducts across the gap. When the displacer moves back, the thermal energy is "shuttled" towards the cold end.

The leakage of gas past the displacer can be simulated with an extra flow path. Simulating the shuttle losses is more difficult. The approach used by the model is to let the mesh of the appendix gap and the cold finger tube move relative to each other. At each time step, the cells are divided into subcells, as shown in Figure 2. The temperatures of the gas and wall subcells are calculated by linearly interpolating the cell temperatures.

The rate of heat transfer is calculated separately for each subcell and the change of energy is applied to the parent cells. The model calculates the rate of heat transfer by using the method suggested by Andersen[3] and recommended by Sauer.[14] A quadratic polynomial is fitted to the

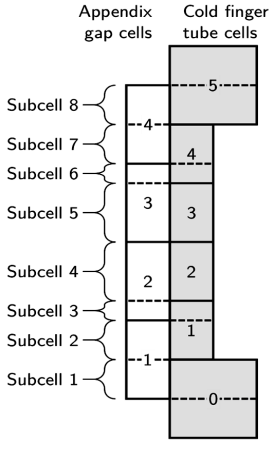

Figure 2. A diagram showing how the appendix gap and cold finger tube are divided into subcells. The solid lines represent the boundaries of the cells. The lengths of the subcells are set so that they do not overlap any cell boundaries. If the cells share the same number, they are in the same row for the energy flow equalisation convergence method. Some subcells span multiple rows so any heat transfer within these is accounted for when calculating the energy flow between rows.

temperatures of the displacer tube wall (T_D), the appendix gap gas (T_g) and the cold finger tube wall (T_F). The thermal gradient of this polynomial at the walls is then used to calculate the rate of heat transfer from the displacer tube and cold finger tube to the gas, given by equations 11 and 12.

$$\dot{Q}_{Dg} = \frac{A_{gs}k}{r}\left(4T_D + 2T_F - 6T_g\right) \tag{11}$$

$$\dot{Q}_{Fg} = \frac{A_{gs}k}{r}\left(4T_F + 2T_D - 6T_g\right) \tag{12}$$

A_{gs} is the surface area of the wall, k is the conductivity of the gas and r is the width of the appendix gap.

Oscillating Flow Correlations

The model makes the assumption that flow through the regenerator mesh, clearance seals and the appendix gap can be modelled using the quasi-static approximation. This is where the heat transfer coefficient and friction factor are calculated using the instantaneous gas properties. This is because the flow channels in these regions are narrow and the steady velocity profiles will develop quickly. This has been shown experimentally.[15]

For gas in variable-volume chambers and ducts, the quasi-static assumption is no longer valid. For these regions, the model uses the oscillating flow correlations that were developed for the Sage model.[4] To enable the use of these correlations, the model tracks the level of turbulence present in these cells. It is also able to simulate heat transfer that is out of phase with the temperature difference and simulate frictional forces that are out of phase with the gas velocity. It does this by phase shifting the temperature and velocity waveforms of the previous cycle and using these in the heat transfer and friction calculations.

MODEL VALIDATION

The model has been validated against single and two-stage Stirling coolers that have been built and tested at RAL.

Single-Stage Cooler Validation

The RAL Small Scale Cooler, shown in Figure 3, was one of the coolers used to validate the model. This compact single-stage Stirling cooler has been developed for use in small satelites.[16] The model was used to replicate a load line where heat loads from 0 W to 1.5 W were applied. Measured temperatures, as well as compressor and displacer motions, were used as inputs into the model; the same cases were also simulated using Sage for comparison.

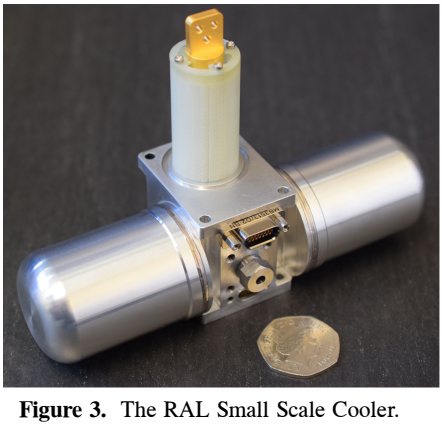

Figure 3. The RAL Small Scale Cooler.

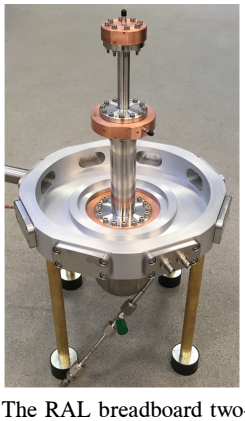

Figure 4. The RAL breadboard two-stage cooler.

It can be seen that both the RAL third-order model and Sage overpredict the cooling power by a similar amount. It is thought that this may be due to the models underestimating the leakage past the compressor clearance seals which have been calculated from the measured sizes of the pistons and bore. Previous measurements taken at RAL have shown that the measured leakage through clearance seals is often higher than is predicted by theory when assuming that the piston and bore are perfect cylinders with the measured diameters. This is the case even when the piston is considered to be fully eccentric within the bore.

The theoretical leakage can be made to agree with the measured leakage by increasing the clearance seal gap by a scale factor. However, it is unclear what scale factor should be used as the required factor has been found to be different for different seals. Increasing the compressor piston and appendix gap clearances seals of the RAL third-order model by 50% gave good agreement with the measured load line. The results can be seen in the right plot of Figure 5. This scale factor is within the range of factors required to match theoretical seal leakages to measured leakages. The gap of the displacer shaft seal was not increased as this gap was calculated from the measured leakage. The calibrated model has good agreement with the measured cooling power over the entire temperature range. This suggests that increasing the clearance seal gaps is a reasonable way of calibrating the model.

The difference in cooling power between the two models appears to be mostly due to the differences in how the appendix gaps are simulated. The RAL third-order model simulates the appendix gap as tapered because the displacer contracts at the cold end. The Sage model assumes a constant gap which is set to the mean of the tapered gap. The constant gap reduces the effectiveness of the seal and increases the enthalpy transport in the appendix gap.

Two-Stage Cooler Validation

The model has also been validated against data from a two-stage cooler. This breadboard two-stage cooler was built specifically to help validate the model and is shown in Figure 4.

Unlike the Small Scale Cooler, the clearance seal leakage was measured for both the compressor piston and displacer shaft clearance seals. This means that a theoretical gap size could be calculated that would give the correct leakage in the model and a scale factor was not required for these seals. However, the leakage was not measured for the appendix gaps. The size of the appendix gaps was calculated from the measured sizes of the displacer and cold finger tube, accounting for thermal contraction. The displacer was assumed to be fully eccentric in the bore.

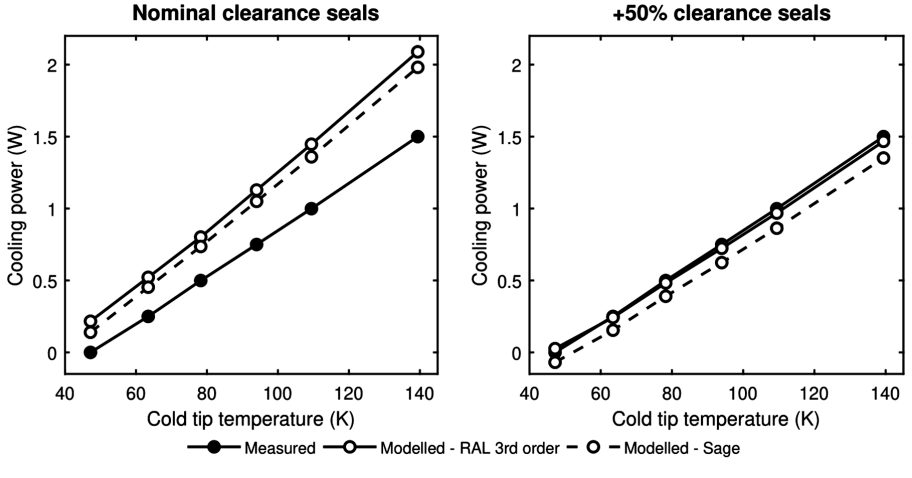

Figure 5. The results of the RAL third-order model and Sage compared to a measured Small Scale Cooler load line. The left plot shows the results of the models with the measured clearance seals. The right plot shows the results of the models with the compressor piston clearance seals and the appendix gap increased by 50%.

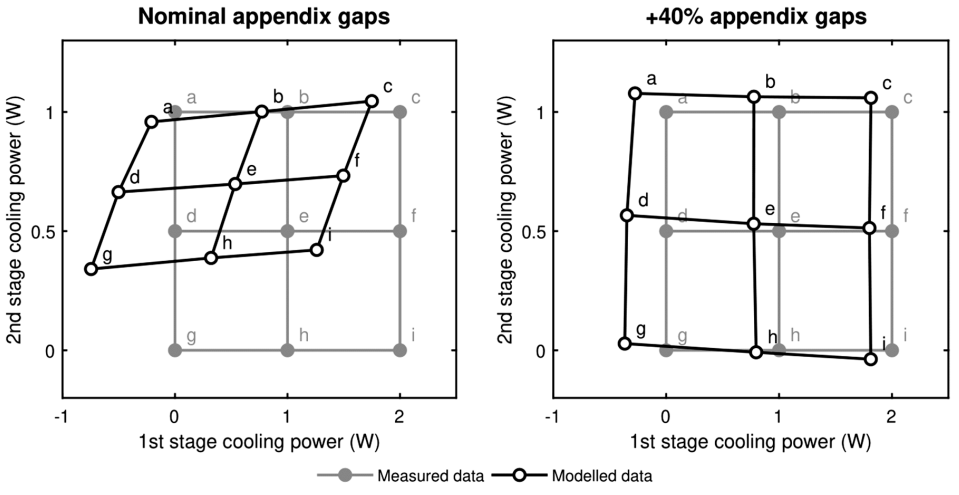

Figure 6. The results of the RAL third-order model when simulating the performance of the breadboard two-stage cooler at a range of temperatures. Each letter correspond to a different case. For example, case "g" has stage temperatures of 59.1 K and 46.4 K for the first and second stages whereas case "c" has stage temperatures of 98.8 K and 99.9 K. The left plot shows the results of the model with the measured appendix gaps and the right plot shows the results of the model with the appendix gaps increased by 40%.

The model was used to replicate a measured load map where different heater powers had been applied to each stage; the measured stage temperatures and compressor and displacer motions were used as inputs into the model. The predicted performance using the measured appendix gaps is shown in the left plot of Figure 6. In addition, a range of clearance seal scale factors for the appendix gaps were investigated, with the same factor being applied to both stages. Increasing the gaps by 40% gave the best agreement and the results are shown in the right plot of Figure 6.

The results show that increasing the size of the appendix gaps greatly improves the accuracy of the model. The larger gaps reduce the modelled cooling power at the second stage because the gas is able to partially bypass the second stage regenerator and transport enthalpy to the cold tip.

Knowing that this calibration factor is required will be invaluable when designing future two-stage coolers. It may result in requiring the displacer to be made from a material with a low coefficient of thermal expansion in order to keep the appendix gap small when the displacer is cold.

MODEL RESULTS

The RAL third-order model works in a similar way to other third-order models in the literature; however, its key feature is that it simulates the entire geometry of the cold finger with cells that interact realistically. These interactions can have a large influence on the modelled performance. Simulating the full geometry allows investigation of aspects of Stirling cooler design that is not possible with other models.

Cold Tip and Displacer Overlap

One aspect of cooler design that can be investigated using the RAL third-order model is how the overlap of the cold tip and the mean displacer position affects the performance. This overlap is shown in Figure 7. Increasing the overlap provides more surface area for the heat transfer to occur which should reduce the temperature difference between the gas and the cold tip. However, it also reduces the length of the cold finger tube, leading to higher thermal conduction. The other key effect is that changing the overlap affects the alignment of the thermal gradients along the displacer and cold finger tube. The shuttle losses are increased if the gradients are not aligned.

Figure 8 shows the effect that changing the overlap would have on the Small Scale Cooler's performance, as predicted by the RAL third-order model. The model predicts that the perfor-

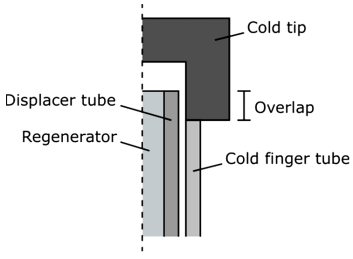

Figure 7. A diagram showing the overlap between the displacer and the cold tip. The overlap is when the displacer is in its mean position.

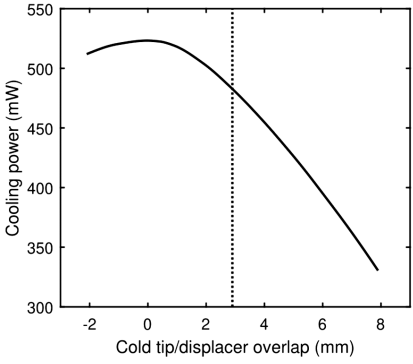

Figure 8. A plot showing the cooling power predicted by the RAL third-order model when the mean cold tip and displacer overlap is adjusted. The other input parameters are taken from the 78 K case of the Small Scale Cooler. The vertical dotted line shows the nominal overlap.

mance can be improved by around 40 mW by reducing the overlap. Making this change aligns the thermal gradients along the cold finger tube and displacer and reduces the shuttle losses.

A similar analysis has been performed at the warm end of the cooler by adjusting the overlap between the cooler body and the warm end of the displacer. It was found that cooling power was not as sensitive to the warm end overlap and the overlap was already near the optimum.

Appendix Gap Geometry

The RAL third-order model is able to simulate coolers where the size of the appendix gap varies along the length of the cold finger. This is often the case for coolers built at RAL; the displacer is typically made from plastic which shrinks more than the metal cold finger tube when cooled, increasing the gap at the cold end. The model was used to investigate the influence a tapered appendix gap has on the Small Scale Cooler's performance.

The results of this investigation are plotted in Figure 9. The tapered gap appears to improve the cooling power at the current gap size by around 90 mW when compared to a constant gap of the same mean size. Because the mean sizes are the same, the shuttle losses should be similar. Therefore, the difference in cooling power is probably due to the reduced seal leakage at the warm end for the tapered gap.

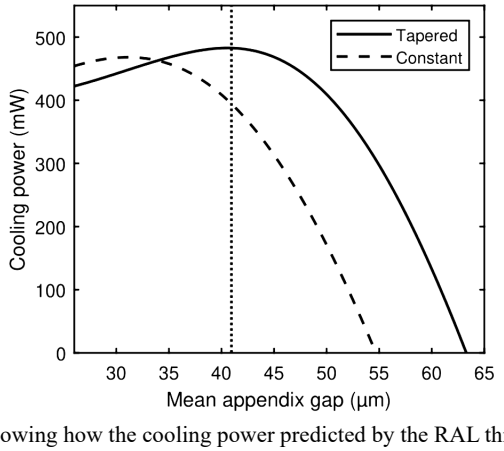

Figure 9. A plot showing how the cooling power predicted by the RAL third-order model is affected by the mean gap size for tapered and constant appendix gaps. The gradient of the tapered gap was fixed and the gap sizes at the warm and cold ends were changed by the same amount. The other input parameters are taken from the 78 K case of the Small Scale Cooler. The vertical dotted line shows the nominal gap size.

CONCLUSION

A new Stirling cryocooler model has been developed that builds on previous models in the literature by simulating the interactions within the entire cold finger. The results of the RAL third-order model are broadly similar to other models in the literature, such as Sage; however, the RAL third-order model is able to investigate aspects of cold finger geometry that are difficult to assess with other models. The results of the model have been validated against performance measurements of coolers taken at RAL. It was found that the model accuracy was improved by using clearance seal gaps that are 40-50% larger than the measured size. This is because the leakage past the seals appears to be greater than is predicted theoretically.

The model will be used to aid the design of future coolers at RAL. Further information about the model will be published in an upcoming PhD thesis.[17]

ACKNOWLEDGEMENT

This work has been funded by the European Research Council under the European Union's Horizon 2020 research and innovation programme (grant agreement: IRIS, no. 648604).

REFERENCES

1. Dyson, R. W., Geng, S. M., Tew, R. C., Adelino, M., "Towards Fully Three-Dimensional Virtual Stirling Convertors For Multi-Physics Analysis and Optimization," *Engineering Applications of Computational Fluid Mechanics*, vol. 2 (2008), pp. 95-118.
2. Urieli, I., *A Computer Simulation of Stirling Cycle Machines*, PhD thesis, University of Witwatersrand (1977).
3. Andersen, S. K., *Numerical Simulation of Cyclic Thermodynamic Processes*, PhD thesis, Technical University of Denmark (2006).
4. Gedeon, D., *Sage User's Guide*, Gedeon Associates, v11 edition (2016).
5. Martini, W. R., *Stirling Engine Design Manual*, United States Department of Energy (1978).
6. Patankar, S., *Numerical Heat Transfer and Fluid Flow*, Taylor & Francis (1980).
7. Lemmon, E.W., Huber, M.L., McLinden, M.O., *NIST Standard Reference Database 23: Reference Fluid Thermodynamic and Transport Properties-REFPROP*, Version 9.1, NIST (2013).
8. Versteeg, H., Malalasekera, W., *An Introduction to Computational Fluid Dynamics: The Finite Volume Method,* 2nd edition, Pearson Education Limited (2007)
9. Courant, R., Friedrichs, K., Lewy, H., "On the Partial Difference Equations of Mathematical Physics," *IBM journal of Research and Development*, vol. 11, issue 2 (1967), pp. 215–234.
10. Shampine, L., Gladwell, I., Thompson, S., *Solving ODEs with MATLAB*, Cambridge University Press (2003).
11. Kühl, H. D., Shulz, S., "Measured Performance of an Experimental Vuilleumier Heat Pump in Comparison to 3rd Order Theory," *Proceedings of the 25th Intersociety Energy Conversion Engineering Conference*, vol. 5 (1990), pp. 436–441.
12. Harvey, J.P., Kirkconnell, C. S., Desai, P. V., "A Fast and Accurate Regenerator Numerical Model," *Cryocoolers 13*, Springer US, Boston, MA (2005), pp. 455–461.
13. Carslaw, H., Jaeger, J., *Conduction of Heat in Solids*, Oxford, Clarendon Press (1959).
14. Sauer, J., Kühl, H. D., Numerical Model for Stirling Cycle Machines Including a Differential Simulation of the Appendix Gap, *Applied Thermal Engineering 111* (2017), pp. 879–833.
15. Gedeon, D., Wood, J. G., *Oscillating-Flow Regenerator Test Rig: Hardware and Theory with Derived Correlations for Screens and Felts*, Tech. rep., Lewis Research Center (1996).
16. Crook, M., Hills, M., Brown, S., Kendall, S., Korswagen, H., Iredale, P., "Small Scale Cooler – Improvements," *Cryocoolers 19*, ICC Press, Boulder CO (2018), pp. 93–101.
17. Rawlings, T., *Numerical Modelling of Stirling Cryocoolers*, PhD thesis, University College London (unpublished).